ISSN 0016-7029, Geochemistry International, 2007, Vol. 45, No. 8, pp. 770–780. © Pleiades Publishing, Ltd., 2007.
Original Russian Text © V.A. Alekseyev, 2007, published in Geokhimiya, 2007, No. 8, pp.842–853.

Equations for the Dissolution Reaction Rates of Montmorillonite, Illite, and Chlorite

V. A. Alekseyev

Vernadsky Institute of Geochemistry and Analytical Chemistry, Russian Academy of Sciences, ul. Kosygina 19, Moscow, 119991 Russia

e-mail: alekseyev-v@geokhi.ru

Received February 22, 2006

Abstract—The available experimental data on the dissolution kinetics of montmorillonite, illite, and chlorite were analyzed. The reliability of the data was assessed and possible reasons for discrepancies were discussed. The dissolution rates of the minerals were described by quantitative and qualitative dependencies on various parameters. The quantitative relations were described by various equations, which were proposed in other studies or derived by the author on the basis of the mathematical processing of the raw data. General equations were obtained for the dissolution rate of each of the minerals as a function of temperature, pH, and the degree of saturation of the solution. For the dependencies that were not constrained by experiments, experimental data for structurally similar minerals or theoretical equations were invoked.

DOI: 10.1134/S0016702907080046

INTRODUCTION

A recent book by Alekseyev et al. [1] summarized the available experimental data on the dissolution kinetics of feldspars, micas, kaolinite, silica, aluminum and iron oxides and hydroxides, olivines, pyroxenes, and amphiboles. This paper updates this list by adding montmorillonite, illite, and chlorite, for which new experimental data were recently published. The kinetic equations and constants obtained by the analysis of these pieces of evidence can be used as reference data for the numerical simulation of various geochemical processes.

METHODS

The rate of mineral dissolution (r) is defined as the number of moles of a mineral passing into the solution per unit surface area and unit time and has a dimension of (mol m^{-2} s^{-1}). Kinetic experiments are carried out using fresh natural mineral samples, which are preliminarily crushed, sieved, and purified from other mineral admixtures and dust particles of the same mineral. The value of r is measured in batch or flow-through reactors. In the former case, r is determined from the slope of kinetic curves in the concentration–time coordinates; in the latter case, it is obtained from the rate of solution filtration and the difference between the concentrations of dissolved elements in the input and output solutions. The second method is more robust because it allows preventing the precipitation of secondary minerals and its influence on r. When necessary, this method can be used to measure r far from equilibrium, where the influence of solution saturation degree is negligible, and provides a means to control the attainment of a steady state.

The steady state is predated by a short initial stage involving the dissolution of surface defects, which were formed during crushing, and remains of dust particles. Nonstoichiometric dissolution occurring during the initial stage results in the formation of a leached surface layer depleted in Na, K, Ca, Mg, and Al and enriched in H (as H^+, H_3O^+, or H_2O) [1]. The transition from the initial to the steady-state stage in a flow-through reactor corresponds to the moment when the concentrations of dissolved elements in the output solution cease to decrease. The goal of kinetic experiments is the measurement of r during this stage.

The uncertainty of r is controlled mainly by the measurement accuracy of the surface area of the mineral. The measured r values are usually normalized to the initial surface area (before the experiment) determined by the adsorption BET method. Such an approach was accepted in the present study. The BET method yields the total surface area accounting for the ruggedness of grain surfaces and pores where water molecules can enter. The surface area of potassium feldspar, albite, and oligoclase may show two- to threefold increases during dissolution, depending on temperature, solution pH, and experiment duration [2, 3]. Taking into account this phenomenon, some authors normalized r to final rather than initial surface areas.

Another approach to the normalization of r values is based on some specific characteristics of dissolution, which occurs mainly on defect areas. This causes the formation of etch pits, which evolve with time into tunnel pores. The total surface area increases at the

Table 1. Starting compositions of montmorillonites used in kinetic experiments

Mineral formula	Reference
$K_{0.02}Na_{0.05}Ca_{0.41}Mg_{0.18}(Al_{2.77}Mg_{1.11}Fe_{0.17})(Si_{7.70}Al_{0.30})O_{20}(OH)_4$	[9]
$K_{0.012}Na_{0.448}Ca_{0.098}(Al_{3.105}Mg_{0.511}Fe_{0.357})(Si_{7.98}Al_{0.02})O_{20}(OH)_4$ $K_{0.04}Ca_{0.50}(Al_{2.8}Mg_{0.7}Fe_{0.53})(Si_{7.65}Al_{0.35})O_{20}(OH)_4$	[10]
$K_{0.19}Na_{0.51}Ca_{0.195}Mg_{0.08}(Al_{2.56}Mg_{1.02}Fe_{0.42})(Si_{7.77}Al_{0.23})O_{20}(OH)_4$	[11]
$K_{0.25}Na_{0.25}Ca_{0.12}Mg_{0.13}(Al_{2.76}Mg_{1.03}Fe_{0.33})(Si_{7.66}Al_{0.34})O_{20}(OH)_4$	[12]
$Na_{0.94}(Al_{2.94}Mg_{0.92}Fe_{0.14})(Si_{7.94}Al_{0.06})O_{20}(OH)_4$ $Na_{0.78}(Al_{2.98}Mg_{0.62}Fe_{0.44})(Si_{7.78}Al_{0.22})O_{20}(OH)_4$	[13]
$K_{0.20}Na_{0.20}Ca_{0.18}Mg_{0.13}(Al_{2.83}Mg_{0.89}Fe_{0.37})(Si_{7.58}Al_{0.42})O_{20}(OH)_4$	[14]
$K_{0.03}Na_{0.11}Ca_{0.33}Mg_{0.10}(Al_{3.06}Mg_{0.83}Fe_{0.16})(Si_{7.68}Al_{0.32})O_{20}(OH)_4$ $Na_{0.77}Ca_{0.08}(Al_{3.00}Mg_{0.59}Fe_{0.40})(Si_{7.68}Al_{0.32})O_{20}(OH)_4$	[15]
$K_{0.636}(Al_{3.018}Mg_{0.566}Fe_{0.41})(Si_{7.95}Al_{0.05})O_{20}(OH)_4$	[16]

expense of the inert side walls of pores, whereas the surface area of active dissolution zones (pore bottoms) remains essentially unchanged. In such a case, it is more reasonable to normalize r to the geometric surface area (r_{GEO}), which is an idealized surface area of smooth spherical or cubic grains, rather than to total surface area (r_{BET}) [4, 5].

Within this approach, the problem of higher r values obtained under laboratory conditions compared with field measurements can in part be overcome. A transition from r_{BET} to r_{GEO} reduces the average discrepancy between the field and laboratory r values from 6 to 4 orders of magnitude [6]. This is explained by the fact that the BET specific surface area of weathered mineral grains is on average two orders of magnitude greater than that of unaltered grains of the same size. The r_{BET} of fresh (unaltered) minerals can be obtained from r_{GEO} using the expression $r_{GEO} = \lambda\ r_{BET}$, where $\lambda = 7–10$ is the surface roughness factor [7, 8]. Phyllosilicates show some peculiarities of predominant dissolution, which are discussed below.

The presentation of data in this paper is accompanied by the assessment of the reliability and the analysis of reasons for the discrepancy between the results of different studies. The presented qualitative expressions were either adopted from other studies or derived by the author during the mathematical processing of raw data. The coefficients of rate equations were calculated by the least squares method or by the Nelder–Mead simplex algorithm implemented in the MatLab software platform. The mechanisms underlying kinetic regularities and possible methods for the derivation of mutually consistent rate equations for various minerals are discussed.

The minimum set of kinetic data for each mineral includes the equations of its dissolution rate as a function of temperature, pH, and solution saturation degree. If there is no experimental evidence for a particular dependency, data on other minerals with similar compositions and structures were invoked. If such data are also missing, average experimental data for mineral groups or theoretical relationships were used.

MONTMORILLONITE

Composition and Surface Area

The compositions of montmorillonites (smectites) used in kinetic experiments are given in Table 1. Montmorillonite differs from micas in having less interlayer cations and showing no three-dimensional ordered structure. The normalization of montmorillonite dissolution rate to surface area (S) poses the problem of accurate measurement of S. According to the data of potentiometric titration and atomic force microscopy, the dissolution of montmorillonite occurs mainly on the edge surface of crystals, S_e [16, 17]. This implies that it would be reasonable to normalize the dissolution rate to S_e. However, direct methods of S_e measurement are too expensive and laborious, and there is no correlation between S_e and the BET surface area (S_{BET}) [17]. The S_{BET} values of montmorillonite vary depending on degassing temperature: an increase in temperature results in a more extensive removal of moisture from microscopic pores, and S_{BET} increases by a factor of 3–4. In order to standardize the measurements, it was proposed to limit the maximum temperature of degassing at 135°C, when the contribution of micropores in the total surface area is no larger than 10%. Another shortcoming is related to S_{BET} changes during the preliminary acid treatment of montmorillonite and during experiments. For instance, dissolution at 50°C and pH 2–3 resulted in up to a fourfold increase in the S_{BET} of montmorillonite, which is explained by the disintegration of particles and an increase in microscopic porosity owing to the removal of interlayer Ca^{2+} [17]. Montmorillonite dissolution at 80°C and pH 8.8 resulted in both an increase and a decrease in S_{BET} [11]. As the experimental methods were identical in both cases (stirred flow-through reac-

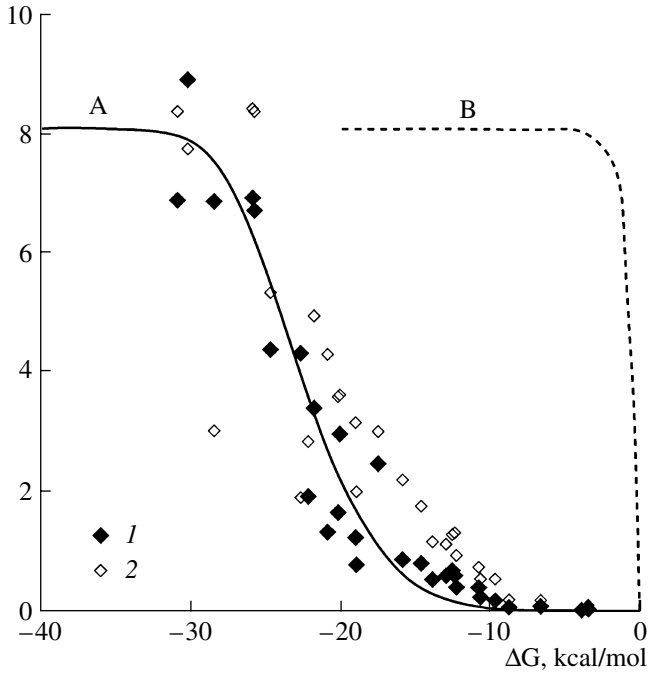

Fig. 1. Dissolution rate of montmorillonite as a function of solution saturation degree at 80°C and pH 8.8 [11]. The symbols show experimental data normalized to BET surface areas measured (*1*) after experiments and (*2*) before experiments. Line A approximates the experimental data by Eq. (1). Line B corresponds to theoretical equation (2).

tors), the difference between the measured S_{BET} values can be attributed to the different solution pH values.

Taking into account the described difficulties, some researchers normalized the dissolution rate of montmorillonite to its mass rather than to its surface area [9, 15, 16]. In this study, the traditional approach was used, i.e., the values of dissolution rate (r) are reported in moles per unit of initial mineral surface measured by the BET method. All molar quantities refer to the formula based on 24 oxygen atoms. The values of r are related to the slow steady-state stage of dissolution, which follows the short initial stage of nonstoichiometric dissolution. During the initial stage, the major portion of interlayer cations is removed into the solution and defects are dissolved. During the steady-state stage, the dissolution of montmorillonite is usually congruent and occurs at a constant rate. Deviations from stoichiometric dissolution were observed in near neutral solutions, when Al and Fe hydroxides were formed [9, 11]. The values of r are usually determined from the rates of Si or Al and Si extraction into the solution.

The influence of montmorillonite composition on r was never systematically explored. The log$r$ values measured in different montmorillonite samples by a single method differ by up to 0.3–0.5 [10, 15]. The stirring of solution has no effect on r values.

Solution Saturation Degree

The influence of the degree of solution saturation on the dissolution rate of montmorillonite at 80°C and pH 8.8 is described by the following equation (Fig. 1):

$$r = k\left\{1 - \exp\left[p\left(\frac{\Delta G}{RT}\right)^q\right]\right\}, \quad (1)$$

where $k = 8.1 \times 10^{-12}$ mol m^{-2} s^{-1}, $p = -6 \times 10^{-10}$, $q = 6$, ΔG is the free energy (quotient) of the reaction, R is the gas constant, and T is the absolute temperature. Equation (1) is empirical and has no physical meaning; i.e., it is not derived from a theoretical model. In contrast to other equations describing the r–ΔG relation, Eq. (1) is fully nonlinear; i.e., r is a nonlinear function of ΔG both under far-from and near-equilibrium conditions. The presented k, p, and q values are not unique. There are several possible combinations of these coefficients describing the experimental data with approximately equal accuracies. The r values normalized to the surface area measured before and after experiments are somewhat different, but these differences show no distinct systematic trends.

The real r–ΔG relation described by Eq. (1) is significantly different from the equation deduced from the transition state theory [18, 19]:

$$r = k[1 - \exp(\Delta G/(RT))]. \quad (2)$$

This can be seen in Fig. 1 from the divergence of lines *A* and *B*. According to the theoretical equation, the plateau of constant r values is reached at $\Delta G < -4$ kcal/mol, whereas the experimental equation gives $\Delta G < -30$ kcal/mol. The real r–ΔG relation can be different at other temperatures and pH values. In particular, this is suggested by the data obtained at various solution filtration rates in the reactor [9]. According to these data, the plateau of r values is reached at 50°C and pH 4 at a lower ΔG value of –20 kcal/mol.

Temperature and pH of Solution

In acid solutions, the dependence of the montmorillonite dissolution rate on temperature (25–70°C) and solution pH (1–4) is described by the Langmuir equation [9]

$$r = A\exp\left(\frac{-E_a}{RT}\right)\left[\frac{K\exp(-\Delta H^0/(RT))a_{H^+}}{1 + K\exp(-\Delta H^0/(RT))a_{H^+}}\right], \quad (3)$$

where E_a is the activation energy of the reaction, ΔH^0 is the enthalpy of adsorption, and a_{H^+} is the activity of H^+ in the solution. The equation is based on the model assuming that the dissolution rate is proportional to the concentration of protons adsorbed on the mineral surface. The experimental data are described by Eq. (3) at $A = 3.33$ mol m^{-2} s^{-1}, $E_a = 17$ kcal/mol, $K = 3 \times 10^{-6}$, and $\Delta H^0 = -11$ kcal/mol.

In alkaline solutions (pH 11.5–14.0), the r–pH dependence is described by the equation $r = ka^n_{OH^-}$ [10]. Within 35–80°C, the order of the reaction ($n = 0.15$) is independent of temperature, and E_a (12.4 kcal/mol) is independent of pH. However, other data obtained at 30–70°C and pH 7–13 indicated an increase in n with increasing temperature, which implies a decrease in E_a with decreasing pH [20]. These data were approximated by the following equation deduced from the model of two parallel adsorption reactions [21]:

$$r = 4.74 \times 10^{-6} \exp\left(\frac{4760}{T}\right)\left(\frac{Ua_{OH^-}}{1 + Ua_{OH^-}}\right) + 1.70\exp\left(\frac{8380}{T}\right)\left(\frac{Va_{OH^-}}{1 + Va_{OH^-}}\right), \quad (4)$$

where $U = 177\exp(2460/T)$ and $V = 0.0297\exp(2830/T)$.

In near neutral solutions (pH 7.5–8.7), the r value of montmorillonite is independent of pH but changes with temperature in accordance with the Arrhenius equation with $E_a = 7.3$ kcal/mol [14]. Huertas et al. [14] argued that the differences between the E_a values in acid, alkaline, and near neutral solutions are not accidental and suggest E_a dependence on solution pH. However, as was noted above, the results of some studies are inconsistent with this conclusion. Therefore, the value of E_a can be considered as constant to a first approximation. This allows us to describe a larger body of experimental data by a single equation. By analogy with other minerals [1], a potentially good master equation can be obtained by combining the Arrhenius equation with a U-shaped dependency of r on solution pH (Fig. 2):

$$r = \exp\left(\frac{-E_a}{RT}\right)(A_{H^+}a^m_{H^+} + A_{H_2O} + A_{OH^-}a^n_{OH^-}). \quad (5)$$

The terms within the second parentheses on the right characterize three dissolution mechanisms prevailing in acid, near neutral, and alkaline solutions. The approximation of 150 triads of experimental T–pH–r values by Eq. (5) yielded the following coefficients: E_a = 9.44 kcal/mol, $A_{H^+} = 1.08 \times 10^{-4}$, $m = 0.764$, $A_{H_2O} = 1.86 \times 10^{-8}$, $A_{OH^-} = 1.08 \times 10^{-5}$, and $n = 0.422$. A change from the U-shaped $\log r$–pH relation described by Eq. (5) to a V-shaped function (at $A_{H_2O} = 0$) did not significantly affect the shape of the curve (Fig. 2) and calculated coefficient: $E_a = 9.34$ kcal/mol, $A_{H^+} = 8.30 \times 10^{-5}$, $m = 0.739$, $A_{OH^-} = 8.78 \times 10^{-6}$, and $n = 0.385$. In both cases, the mean square deviation of the experimental $\log r$ values from the calculated curves is 0.26. The second variant (with $A_{H_2O} = 0$) is more favorable as it includes a smaller number of adjusted parameters.

Several experiments denoted in Fig. 2 by open symbols were not used in mathematical processing. These are the data of [16, 22] obtained at 25°C and pH 1–5 in 0.03 and 0.1 M KCl solutions, respectively. They are consistent with each other but differ from other data in a shallower slope of $\log r$/pH. The differences could be due to the shortcomings of methods related to the incongruent character of dissolution (insufficient run duration) and different r values obtained in batch and flow-through reactors. Similar to the degree of incongruency, these differences change regularly with pH variations.

The data of Cama et al. [11] obtained at 80°C and pH 8.8 as well as those of Sato et al. [20] for 30–70°C and pH 7–13 were also rejected during the mathematical treatment. They show overestimated r values, and the magnitude of overestimation increases with decreasing pH (Fig. 2). The reliability of Sato et al.'s [20] data is difficult to assess, because the details of their methods were not given. As to the data of Cama et al. [11], they are related to montmorillonite with the maximum content of interlayer cations (Table 1); i.e., it is possible that the composition of the mineral affected the rate of its dissolution.

Other Kinetic Parameters

Zysset and Schindler [16] reported an increase in the dissolution rate of montmorillonite, r, with increasing KCl concentration in the solution at pH 1–4: in 1 M KCl solution, r was an order of magnitude higher than in 0.1 M solution and two orders of magnitude higher than in 0.03 M solution. This effect was explained by the model suggesting that r is proportional to the concentration of protons adsorbed on the mineral surface. The adsorption of protons involves two parallel reactions: (1) protonation of surface aluminol groups $> AlOH_2^+$ and (2) ion exchange with interlayer potassium. The model is in agreement with the experimental data for 0.03 and 0.1 M KCl solutions but is inconsistent (underestimates r) with the data for 1.0 M KCl solution. The low reliability of experimental data on the r–m_K relation is indicated by the identical $\log r$ values obtained in two studies [16, 22] for the same montmorillonite samples at different KCl concentrations (0.03 and 0.1 M).

Zysset and Schindler [16] detected some decrease in montmorillonite dissolution rate as Al concentration in the solution increased from 0 to 10^{-4} M. The maximum effect (up to a factor of 3) was observed at pH 4 in a 0.03 M KCl solution and was explained by Al adsorption on edge surfaces, which resulted in the blocking of active dissolution sites. Amram and Ganor [9] did not observe the influence of Al or Si on r within the same pH range ($HNO_3 + NaNO_3$ solutions). Bauer and Berger [10] also failed to detect such an effect in alkaline KOH solutions. The influence of Na^+ and NO_3^- on r is very small (if any) [9].

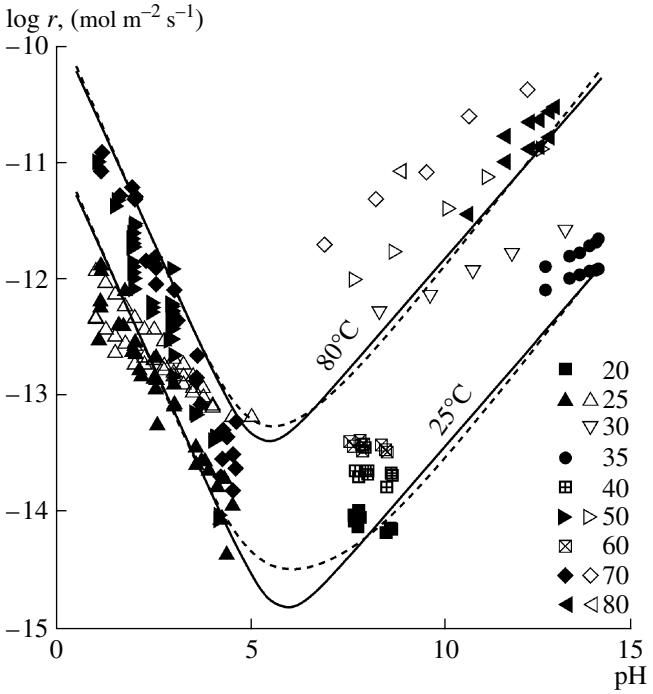

Fig. 2. Dissolution rate of montmorillonite as a function of temperature and solution pH. The symbols show experimental data [9–11, 14–16, 20, 22, 23] obtained at different temperatures (°C). The solid and dashed lines correspond to Eq. (5) at $A_{H_2O} = 0$ and $A_{H_2O} = 1.86 \times 10^{-8}$, respectively. The open symbols indicate the experiments that were not used in mathematical processing.

Transformation of Montmorillonite to Illite (Mnt ⟶ Ill)

We considered above the kinetics of the congruent or near-congruent stage of dissolution, when secondary minerals do not form or form in small amounts. Let us consider the kinetics of the following stage of incongruent dissolution, when illite is formed as a secondary mineral (*Mnt* ⟶ *Ill*). This reaction proceeds at a significant rate, which can be measured in the laboratory, and under a higher temperature than the reaction of congruent montmorillonite dissolution considered above. In near neutral solutions, the occurrence of the *Mnt* ⟶ *Ill* reaction was detected only at temperatures of higher than 120°C [12, 24–27]. In strongly alkaline solutions (0.1–3.0 M KOH or NaOH), the *Mnt* ⟶ *Ill* reaction may be observed already at 60 and even 35°C [13]. However, the dissolution of other montmorillonite samples under the same conditions was not accompanied by the formation of illite layers [10].

The rate of the *Mnt* ⟶ *Ill* reaction is usually determined from the data of X-ray phase analysis or from the rate of silica release into the solution. The amount of illite depends on the association of other newly formed minerals. For instance, montmorillonite of the ideal composition $K_{0.33}Al_2(Si_{3.67}Al_{0.33})O_{10}(OH)_2$ (*Mnt*) can be transformed either to pure illite, $K_{0.8}Al_2(Si_{3.2}Al_{0.8})O_{10}(OH)_2$ (*Ill*), or to illite and kaolinite, $Al_2Si_2O_5(OH)_4$ (*Kln*):

$$1.2Mnt + 0.4K^+ + 2.4H_2O = Ill + 1.2H_4SiO_4^0 + 0.4H^+, \quad (6)$$

$$2.4Mnt + 7H_2O = Ill + Kln + 2.8\ H_4SiO_4^0. \quad (7)$$

The formation of one mole of illite requires the extraction of silica into the solution, 1.2 moles in the former case and 2.8 moles in the latter case. The stoichiometry of the reactions implies that reaction (6) occurs only in K^+-bearing solutions, whereas reaction (7) can occur in pure water.

Under laboratory conditions, the *Mnt* ⟶ *Ill* reaction occurs only with dioctahedral montmorillonite. Trioctahedral montmorillonite (saponite) does not change in water up to a temperature of 500°C [27]. During the *Mnt* ⟶ *Ill* reaction, an increase in potassium content in the interlayer sites is accompanied by the substitution of silicon for aluminum in the tetrahedral sites and/or aluminum for magnesium in the octahedral sites [26, 28, 29]. These substitutions may proceed via diffusion, i.e., without the destruction of the mineral lattice [25, 30], or via montmorillonite dissolution and illite precipitation from the solution [31]. Both of the mechanisms may operate concurrently.

The rate of the *Mnt* ⟶ *Ill* reaction increases with increasing temperature after montmorillonite saturation in potassium and with increasing potassium content in the solution [27, 28, 32]. In potassium-bearing solutions, the rate of the *Mnt* ⟶ *Ill* reaction decreases with increasing contents of Na, Ca, and Mg in the solution [25, 30].

The rate of the *Mnt* ⟶ *Ill* reaction in water (kaolinite and quartz are also formed as secondary minerals) is described by the following equations at 260–390°C [26]:

$$\ln\left(\frac{1}{F}\right) = k\mathrm{t}, \quad (8)$$

$$k = A\exp\left(\frac{-E_a}{RT}\right), \quad (9)$$

where F is the fraction of montmorillonite in the montmorillonite–illite mixture, k is the constant (day^{-1}), t is the time (day), $A = 1.17 \times 10^5$, and $E_a = 19.5$ kcal/mol.

The rate of the same reaction in near neutral (pH 5.5–7.5) KCl solutions (0.025–1.0*m*) at 120–200°C is described by the equation [12]

$$-\mathrm{d}F/\mathrm{dt} = km^{0.25}F^n, \quad (10)$$

where F, t, and k are the same parameters as in Eq. (8), and m is the concentration of potassium in the solution (mol/kg). The exponent n is poorly constrained. The following integrated forms of Eq. (10) are obtained for possible extreme n values of 1 and 5 at the initial absence of illite:

$$\ln F = -km^{0.25}\mathrm{t}, \quad (11)$$

and

$$1/F^4 = 4km^{0.25}\mathrm{t}. \quad (12)$$

The values of k in Eqs. (11) and (12) are defined by Arrhenius equation (9) at $A = 0.0732$ and $E_a = 7.15$ kcal/mol. Using previous experimental data and a comparison with field observations, Cuadros and Linares [12] argued that the value $n = 5$ is more probable. In order to check this inference, compare the time of montmorillonite replacement by illite according to Eqs. (8), (11), and (12) under identical conditions: a final degree of replacement of 50% ($F = 0.5$), a temperature of 200°C, and a K concentration in the solution of 0.025 *m*. The calculated time is 16, 130, and 750 yr, respectively. Equation (8) is in better agreement with Eq. (11) ($n = 1$) than with Eq. (12) ($n = 5$), which is at odds with the conclusion of [12]. The values of E_a (7.15 and 19.5 kcal/mol) suggest that the r–T dependence is much less pronounced at 120–200°C than at 260–390°C. This difference can be related either to a change in the reaction mechanism or to different methods of the estimation of reaction progress (on the basis of the analysis of solution and solid phase). Moreover, the extrapolation of rate equations for the *Mnt* ⟶ *Ill* reaction beyond the experimentally studied region is very unreliable because these equations are purely empirical and have no physical meaning.

Summary and Recommendations

The general equation for the rate of congruent montmorillonite dissolution can be obtained by combining Eqs. (1) and (5) at $A_{H_2O} = 0$:

$$r = \exp\left(\frac{-E_a}{RT}\right)(A_{H^+}a_{H^+}^m + A_{OH^-}a_{OH^-}^n)\left\{1 - \exp\left[p\left(\frac{\Delta G}{RT}\right)^q\right]\right\}, \quad (13)$$

where $E_a = 9.34$ kcal/mol, $A_{H^+} = 8.30 \times 10^{-5}$, $m = 0.739$, $A_{OH^-} = 8.78 \times 10^{-6}$, $n = 0.385$, $p = -6 \times 10^{-10}$, $q = 6$, ΔG is the free energy (quotient) of the reaction, R is the gas constant, and T is the absolute temperature. Such a combination implies that Eq. (1), which was derived at 80°C and pH 8.8, is valid for the whole interval of temperature (20–80°C) and pH values (1–14).

Although the influence of potassium content in the solution on r can be significant, it is ignored because of the lack of quantitative data. The effects of Al, Si, Na, and inorganic ligands in the solution are also ignored because they are very small or negligible. There is no evidence in the literature on the influence of organic ligands on r.

The kinetics of the *Mnt* ⟶ *Ill* reaction can be described by Eq. (10) at a low temperature (120–200°C) and Eq. (8) at higher temperatures (260–390°C). However, these equations have no physical meaning and are poorly consistent with each other. In addition, their dimensions (fractions) differ from the universally accepted dimension used in kinetic studies (mol m^{-2} s^{-1}).

ILLITE

There is only one comprehensive kinetic investigation of illite dissolution [33]. The dissolution rate of illite, $(Ca_{0.01}Na_{0.13}K_{0.53})(Al_{1.27}Fe^{3+}_{0.36}Mg_{0.44})(Si_{3.55}Al_{0.45})O_{10}(OH)_2$, was studied at 5–50°C in 0.1 *m* NaCl solutions with the addition of HCl, NaOH, H_3CCOOH, NH_3, and $NaHCO_3$ for providing different pH values (1.4–12.4). Köhler et al. [33] approximated these experimental data by the equation

$$r = A_{H^+}\exp\left(\frac{-E_{a,H^+}}{RT}\right)a_{H^+}^m + A_{H_2O}\exp\left(\frac{-E_{a,H_2O}}{RT}\right) + A_{OH^-}\exp\left(\frac{-E_{a,OH^-}}{RT}\right)a_{OH^-}^n \quad (14)$$

the coefficients of which are given in the second column of Table 2. The dashed lines in Fig. 3 were calculated by Eq. (14) using these coefficients for 5 and 50°C. It can be seen that they systematically deviate from the experimental data in the alkaline pH region. My approximation of the experimental data of [33] using the same equation yielded other values for the coefficients (column 3 in Table 2). They correspond to the solid lines in Fig. 3, which are more consistent with the experimental data.

Equation (14) differs from other similar equations in that different E_a values are used for acid, near neutral, and alkalic solutions. In order to estimate how important this modification is, the same data were approximated by Eq. (5), which is an analog of Eq. (14) at $E_{a,H^+} = E_{a,H_2O} = E_{a,OH^-} = E_a$. Two variants of Eq. (5) were used with different $\log r$–pH dependencies: (1) V-shaped ($A_{H_2O} = 0$) and (2) U-shaped ($A_{H_2O} \neq 0$. The coefficients of Eq. (5) for these variants are given in columns 4 and 5 of Table 2. The latter variant gives a better agreement with the experimental data (Fig. 4). Compare now the best variants of Eqs. (14) and (5), i.e., columns 3 and 5 in Table 2. The two equations yield similar mean square deviations between the calculated and measured $\log r$ values. Nonetheless, column 5 is favored as a model with fewer adjustable parameters.

Secondary minerals were never detected in illite dissolution experiments; however, according to thermodynamic calculations, near neutral and alkaline solutions are oversaturated in gibbsite, kaolinite, and brucite.

The results of mathematical processing described above were obtained ignoring r measurements at 20°C, because they were 2–3 times higher than the r values for 25°C [33]. This anomaly is explained by the shorter duration of the 20°C experiments. It was subsequently found that the dissolution rate of illite decreases contin-

Table 2. Coefficients of Eqs. (14) and (5) describing the experimental data [33] on the kinetics of illite dissolution

Coefficient	Equation (14), Fig. 3		Equation (5), Fig. 4	
	Data of [33], dashed line	This study, solid line	$A_{H_2O} = 0$, dashed line	$A_{H_2O} \neq 0$, solid line
1	2	3	4	5
A_{H^+}, mol m^{-2} s^{-1}	2.2×10^{-4}	1.52×10^{-5}	1.65×10^{-7}	1.58×10^{-6}
A_{H_2O}, mol m^{-2} s^{-1}	2.5×10^{-13}	1.29×10^{-11}	0	8.09×10^{-10}
A_{OH^-}, mol m^{-2} s^{-1}	0.27	6.82×10^{-7}	1.87×10^{-7}	1.01×10^{-6}
m	0.6	0.592	0.369	0.586
n	0.6	0.747	0.592	0.760
E_{a, H^+}, kcal/mol	10.99	9.48	–	–
E_{a, H_2O}, kcal/mol	3.35	5.72	–	–
E_{a, OH^-}, kcal/mol	16.01	7.95	–	–
E_a, kcal/mol	–	–	7.62	8.15
Mean square deviation σ*	0.28	0.15	0.24	0.16

* $\sigma = \sqrt{\frac{\sum(\Delta \log r)^2}{n-1}}$, where $\Delta \log r$ is the difference between the logarithms of measured and calculated r values, and n is the number of measurements of the t°C–pH– $\log r$ triads.

uously with time and did not attain a stable value even in five months [34]. The specific surface area of illite does not change significantly during dissolution. A model was proposed to explain these observations, assuming that the edge surface of phyllosilicates is primarily dissolved, and its area decreases during dissolution much more rapidly than the total BET surface area measured. Therefore, additional investigations of the time dependence of the dissolution rate of clay minerals are needed for a more accurate extrapolation of experimental data to natural processes.

The dependence of illite dissolution rate on solution saturation state was never experimentally explored; however, if necessary, a respective dependency determined for the dissolution of another phyllosilicate can be used. Micas are most similar to illite in terms of composition and structure. However, the r–ΔG relations of micas were also not experimentally studied. A less appropriate proxy for illite is montmorillonite, the r–ΔG dependence of which is described by Eq. (1). Combining this equation with Eq. (14) at $E_{a, H^+} = E_{a, H_2O} = E_{a, OH^-} = E_a$ yields

$$r = \exp\left(\frac{-E_a}{RT}\right)(A_{H^+}a_{H^+}^m + A_{H_2O} + A_{OH^-}a_{OH^-}^n)\left\{1 - \exp\left[p\left(\frac{\Delta G}{RT}\right)^q\right]\right\}. \quad (15)$$

The coefficients p and q of this equation are the same as in Eq. (1), and other coefficients are given in column 5 of Table 2.

CHLORITE

The compositions of chlorites used in kinetic experiments are given in Table 3. The dissolution rate of

Table 3. Starting compositions of chlorites used in kinetic experiments

Mineral formula	Reference
$(Al_{1.05}Fe^{3+}_{0.22}Fe^{2+}_{0.27}Mg_{4.34})(Si_{2.98}Al_{1.02})O_{10}(OH)_8$	[35]
$(Al_{0.71}Fe^{2+}_{0.54}Mg_{4.94})(Si_{2.88}Al_{1.12})O_{10}(OH)_8$	[36]
$(Al_{0.84}Fe^{3+}_{0.15}Mn_{0.52}Mg_{4.72})(Si_{2.54}Al_{1.46})O_{10}(OH)_8$	
$(Al_{1.0}Fe_{0.6}Mg_{4.2})(Si_{2.7}Al_{1.3})O_{10}(OH)_8$	[37]
$(Al_{0.9}Fe^{2+}_{0.1}Fe^{3+}_{0.1}Mg_{4.9})(Si_3Al)O_{10}(OH)_8$	[38]
$(Al_{1.31}Fe_{1.97}Mg_{2.68})(Si_{2.78}Al_{1.23})O_{10}(OH)_8$	[39]
$(Al_{1.259}Fe^{2+}_{1.95}Mg_{2.80})(Si_{2.75}Al_{1.25})O_{10}(OH)_8$	[40]
$(Al_{1.24}Fe^{2+}_{1.51}Fe^{3+}_{0.47}Mg_{4.9})(Si_{2.66}Al_{1.33})O_{10}(OH)_8$	[41]
$(Al_{0.84}Fe^{2+}_{0.36}Mg_{4.9})(Si_{3.25}Al_{0.7}Fe^{3+}_{0.06})O_{10}(OH)_8$	[42]
$(Al_{0.97}Fe^{2+}_{1.9}Fe^{3+}_{0.07}Mg_{2.76})(Si_{2.48}Al_{1.52})O_{10}(OH)_8$	[43]
$(Al_{0.7}Fe^{2+}_{0.1}Fe^{3+}_{0.1}Mg_{4.9})(Si_{3.5}Al_{0.5})O_{10}(OH)_8$	[44]

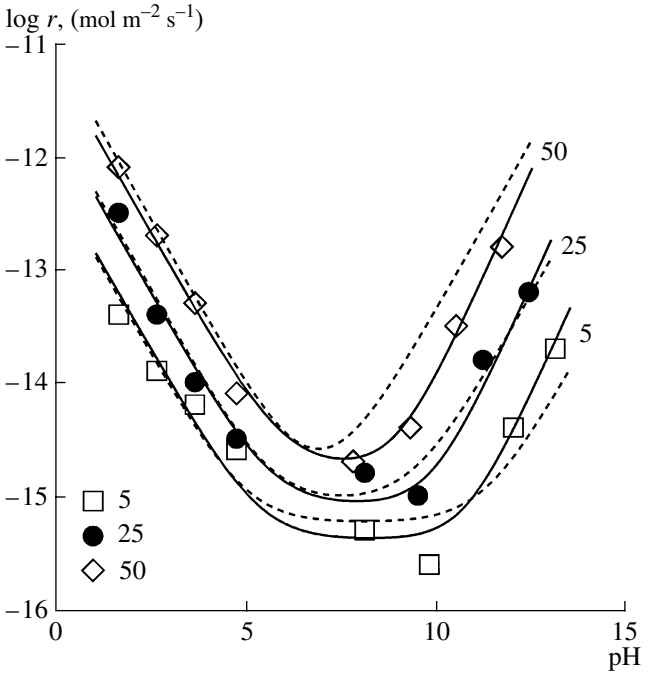

Fig. 3. Dissolution rate (r) of illite as a function of solution pH. The symbols show experimental data [33] obtained at 5, 25, and 50°C. The lines were calculated using Eq. (14) with coefficients given in columns 2 (dashed lines) and 3 (solid lines) of Table 2.

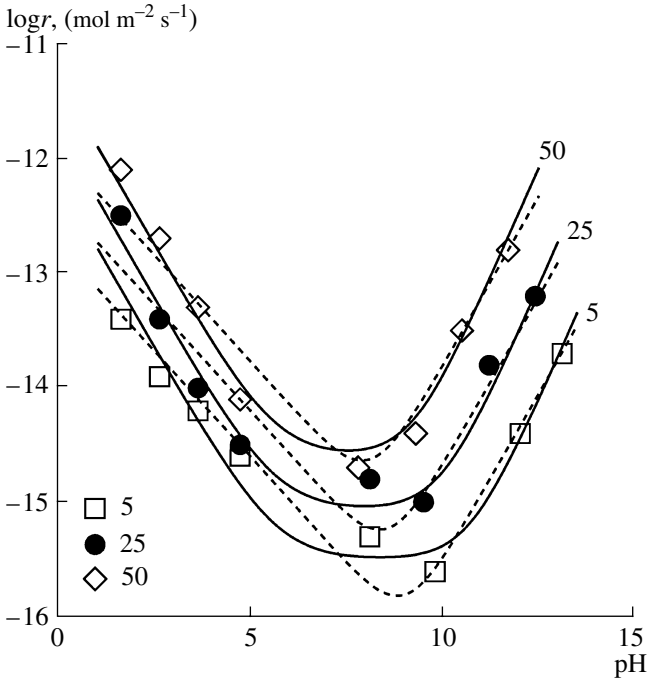

Fig. 4. Dissolution rate (r) of illite as a function of solution pH. The symbols show experimental data [33] obtained at 5, 25, and 50°C. The lines were calculated using Eq. (5) with coefficients given in columns 4 (dashed lines) and 5 (solid lines) of Table 2.

chlorites (r) was experimentally measured at room temperature only. The measurements were conducted in solutions with varying pH values, far from the conditions of chlorite–solution equilibrium. Steady-state dissolution was attained in 5–10 days. The character of steady-state dissolution depends on the pH of solution (Fig. 5), being congruent at pH 1–5 and incongruent (possible formation of Fe, Al, and Mg hydroxides) at pH > 5. Congruent chlorite dissolution was observed in very acid solutions (0.5 N HCl) [45, 46]. The in situ investigations of chlorite dissolution by means of an atomic force microscope showed that, in contrast to other phyllosilicates, the basal surface of chlorite is dissolved much more rapidly than the edges surface [41]. Its layer-by-layer dissolution is controlled by defects (compositional heterogeneities and fractures). The active surface (molecular steps) accounts for only 0.2% of the total surface measured by the BET method. Nonetheless, in order to maintain the unified description of kinetic data, the dissolution rate of chlorite is hereafter expressed in moles of the mineral per unit area of its total surface. The molar amount of chlorite was determined from the rate of Si extraction into the solution taking into account the content of Si in chlorite (the calculated chlorite formula contains 10 O atoms and 8 OH groups; Table 3).

The available experimental data on the dependence of r on the pH value of solution at room temperature were approximated by the equation [43]

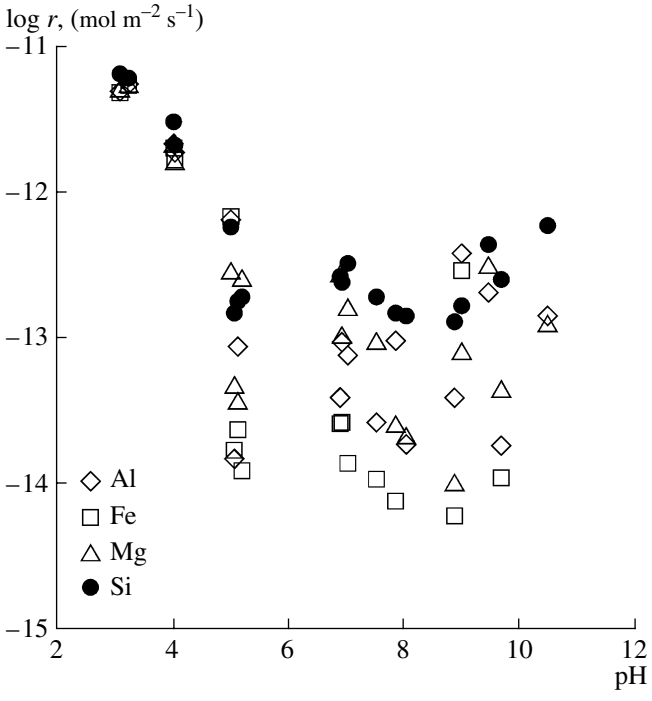

Fig. 5. Dissolution rates of chlorite determined from the rate of Al, Fe, Mg, and Si extraction into the solution depending on solution pH at 25°C [43].

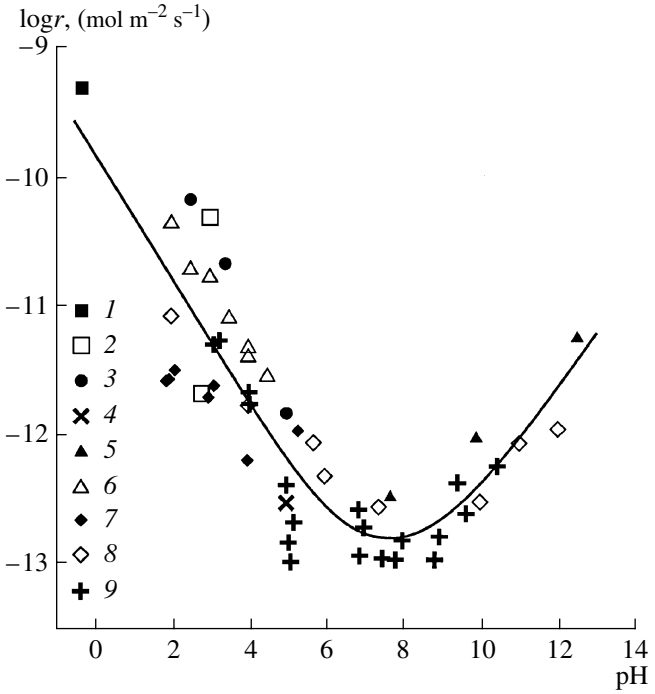

Fig. 6. Dissolution rate (r) of chlorite as a function of solution pH at 25°C. The values of r were determined from the rate of Si extraction into the solution. The symbols show experimental data: (*1*) [35], (*2*) [36], (*3*) [37], (*4*) [38], (*5*) [39], (*6*) [40], (*7*) [41], (*8*) [42], and (*9*) [43]. The line corresponds to Eq. (16) at $k_{H^+} = 1.62 \times 10^{-10}$, $k_{H_2O} = 10^{-13}$, $k_{OH^-} = 1.70 \times 10^{-11}$, $m = 0.49$, and $n = 0.43$.

$$r = k_{H^+}a_{H^+}^m + k_{H_2O} + k_{OH^-}a_{OH^-}^n. \quad (16)$$

The experimental and calculated data show adequate agreement (Fig. 6), especially taking into account the differences in experimental methods, chlorite compositions, and solution chemistry. The data of [44, 47] were not used in the mathematical treatment because they deviate from the general trend by about an order of magnitude. The data of Lowson et al. [43] were also described by the equation

$$r = 10^{-10.46}(a_{H^+}^3/a_{Al^{3+}})^{0.27}. \quad (17)$$

This equation reflects the possible influence of dissolved aluminum (in addition to pH) on the dissolution rate of chlorite. However, the correlation coefficient of $\log r$ with $\log(a_{H^+}^3/a_{Al^{3+}})$ is rather low (0.88), which may indicate that this influence is minor. Additional experiments at a fixed pH value and variable Al content in the initial solution are needed to clarify this effect.

The data shown in Fig. 6 were obtained for inert buffer solutions containing phthalates, phosphates, tris(hydroxymethyl)-aminomethane, hydrochloric acid, chloric acid, sulfuric acid, boric acid, KCl, NaCl, NaOH, and $NaHCO_3$. The addition of these components to solutions exerts a minor effect on r values. Borax (0.0125 M) and oxalate (0.1 M) increase r by a factor of 3 and 10, respectively [43]. In the presence of fulvic acid, the dissolution of chlorite is accelerated by a factor of 2–5 [36]. If the r value of chlorite in a hydrochloric acid solution (pH 1.5–4.5) is taken to be 1, other acids form the following sequence of increasing r: nitric, 0.97; acetic, 1.01; sulfuric, 1.19; citric, 2.7; and oxalic, 3.3 [40].

There is no experimental data on the r–T and r–ΔG relations for the kinetics of chlorite dissolution. By analogy with other minerals, it can be assumed that the r–T dependence of chlorite can also be described by the Arrhenius equation (5). The E_a value of chlorite in this equation can be taken, as a first approximation, to be 17 kcal/mol, which is the average E_a value for all silicates [1]. The r–ΔG dependence of chlorite can be approximated, as a first approximation, by theoretical Eq. (2). Given these assumptions, Eq. (16) can be rewritten as

$$r = \exp\left(\frac{-E_a}{RT}\right)(A_{H^+}a_{H^+}^m + A_{H_2O} + A_{OH^-}a_{OH^-}^n)\left[1 - \exp\left(\frac{\Delta G}{RT}\right)\right], \quad (18)$$

where E_a = 17 kcal/mol, $A_{H^+} = 468$, $A_{H_2O} = 0.289$, $A_{OH^-} = 49.1$, $m = 0.49$, and $n = 0.43$. The values of a_{H^+} and a_{OH^-} in this and similar equations are determined from the pH value of solution and the dissociation constant of water, K_W [48]:

$$a_{H^+} = 10^{-pH}, \quad (19)$$

$$a_{OH^-} = 10^{pH + \log K_W}, \quad (20)$$

$$\log K_W = 5.941 - 0.016638T - 4466.2/T. \quad (21)$$

CONCLUSIONS

The dissolution rates of minerals (r, mol m^{-2} s^{-1}) are experimentally measured in batch or flow-through reactors during the steady-state stage of dissolution after a short initial stage, when dust particles and surface defects are dissolved, and a surface leached layer depleted in alkaline and calc-alkaline elements is formed. The main uncertainty in r values comes from the surface area of minerals, which is measured by the BET method (r_{BET}) or calculated from grain sizes (r_{GEO}). It would be more reasonable to normalize r to actively dissolved surface area (pore bottoms, edge surface, and molecular steps), but this parameter is difficult to measure. Therefore, in order to standardize measurements, the dissolution rates of minerals are usually normalized to their total initial surfaces measured by the BET method.

Published experimental studies on the dissolution kinetics of montmorillonite, illite, and chlorite were

analyzed. Each mineral was characterized by the minimum set of kinetic data, including the equation of dissolution rate as a function of temperature (T), pH, and degree of solution saturation (ΔG). The equations for montmorillonite are based on experimental data. There is no experimental data for the r–ΔG relation of illite and r–T and r–ΔG relations of chlorite. These gaps were filled by experimental data on similar minerals or theoretical equations. As a result, Eqs. (13), (15), and (18) were proposed for the description of the dissolution kinetics of montmorillonite, illite, and chlorite, respectively.

ACKNOWLEDGMENTS

This study was financially supported by the Russian Foundation for Basic Research, project no. 06-05-64110.

REFERENCES

1. V. A. Alekseyev, B. N. Ryzhenko, S. L. Shvartsev, et al., *Geologic Evolution and Self-Organization of the Water–Rock System Vol. 1. Water–Rock System in the Earth's Crust: Interaction, Kinetics, Equilibrium, and Modeling* (SO RAN, Novosibirsk, 2005) [in Russian].
2. Y. Chen and S. L. Brantley, "Temperature- and pH-Dependence of Albite Dissolution Rate at Acid pH," Chem. Geol. **135**, 275–290 (1997).
3. L. L. Stillings and S. L. Brantley, "Feldspar Dissolution at 25°C and pH 3: Reaction Stoichiometry and the Effect of Cations," Geochim. Cosmochim. Acta **59**, 1483–1496 (1995).
4. L.-M. Gautier, E. H. Oelkers, and J. Schott, "Are Quartz Dissolution Rates Proportional to B.E.T. Surface Areas?," Geochim. Cosmochim. Acta **65**, 1059–1070 (2001).
5. A. F. White, A. E. Blum, M. S. Schulz, et al., "Chemical Weathering Rates of a Soil Chronosequence on Granitic Alluvium: I. Quantification of Mineralogical and Surface Area Changes and Calculation of Primary Silicate Reaction Rates," Geochim. Cosmochim. Acta **60**, 2533–2550 (1996).
6. A. F. White and S. L. Brantley, "The Effect of Time on the Weathering of Silicate Minerals: Why Do Weathering Rates Differ in the Laboratory and Field?," Chem. Geol. **202**, 479–506 (2003).
7. A. F. White and M. L. Peterson, "Role of Reactive Surface Area Characterization in Geochemical Models," in *Chemical Modeling of Aqueous Systems II*, Ed. by D. C. Melchior and R. L. Bassett, Am. Chem. Soc. Symp. Ser. **416**, 461–475 (1990).
8. A. F. White, "Chemical Weathering Rates of Silicate Minerals in Soils," in *Chemical Weathering Rates of Silicate Minerals*, Ed. by A. F. White and S. L. Brantley, Rev. Mineral. **31**, 407–461 (1995).
9. K. Amram and J. Ganor, "The Combined Effect of pH and Temperature on Smectite Dissolution Rate under Acidic Conditions," Geochim. Cosmochim. Acta **69**, 2535–2546 (2005).
10. A. Bauer and G. Berger, "Kaolinite and Smectite Dissolution Rate in High Molar KOH Solutions at 35° and 80°C," Appl. Geochem. **13**, 905–916 (1998).
11. J. Cama, J. Ganor, C. Ayora, and C. A. Lasaga, "Smectite Dissolution Kinetics at 80°C and pH 8.8," Geochim. Cosmochim. Acta **64**, 2701–2717 (2000).
12. J. Cuadros and J. Linares, "Experimental Kinetic Study of the Smectite-to-Illite Transformation," Geochim. Cosmochim. Acta **60**, 439–453 (1996).
13. D. D. Eberl, B. Velde, and T. McCormick, "Synthesis of Illite–Smectite from Smectite at Earth Surface Temperatures and High pH," Clay Miner. **28**, 49–60 (1993).
14. F. J. Huertas and E. Caballero, C. Jiménez de Cisneros, et al., "Kinetics of Montmorillonite Dissolution in Granitic Solutions," Appl. Geochem. **16**, 397–407 (2001).
15. V. Metz, K. Amram, and J. Ganor, "Stoichiometry of Smectite Dissolution Reaction," Geochim. Cosmochim. Acta **69**, 1755–1772 (2005).
16. M. Zysset and P. W. Schindler, "The Proton Promoted Dissolution Kinetics of K-Montmorillonite," Geochim. Cosmochim. Acta **60**, 921–931 (1996).
17. V. Metz, H. Raanan, H. Pieper, et al., "Towards the Establishment of a Reliable Proxy for the Reactive Surface Area of Smectite," Geochim. Cosmochim. Acta **69**, 2581–2591 (2005).
18. P. Aagaard and H. C. Helgeson, "Thermodynamic and Kinetic Constraints on Reaction Rates among Minerals and Aqueous Solutions. I. Theoretical Considerations," Am. J. Sci. **282**, 237–285 (1982).
19. A. C. Lasaga, "Chemical Kinetics of Water–Rock Interaction," J. Geophys. Res. **89**, 4009–4025 (1984).
20. T. Sato, M. Kuroda, S. Yokoyama, et al., "Dissolution Kinetics of Smectite under Alkaline Conditions," in *Clays in Natural and Engineered Barriers for Radioactive Waste Confinement. Int. Meeting, March, 14–18, Tours, France* (2005), pp. 19–20.
21. J. Cama, V. Metz, and J. Ganor, "The Effect of pH and Temperature on Kaolinite Dissolution Rate under Acidic Conditions," Geochim. Cosmochim. Acta **66**, 3913–3926 (2002).
22. G. Furrer, M. Zysset, and P. W. Schindler, "Weathering Kinetics of Montmorillonite: Investigations in Batch and Mixed-Flow Reactors," in *Geochemistry of Clay–Pore Fluid Interaction*, Ed. by D. A. C. Manning, P. L. Hall, and C. R. Hughes (Chapman & Hall, London, 1993), Vol. 4, pp. 243–262.
23. H. Hayashi and M. Yamada, "Kinetics of Dissolution of Noncrystalline Oxides and Crystalline Clay Minerals in a Basic Tiron Solution," Clays Clay Miner. **38**, 308–314 (1990).
24. N. I. Khitarov and V. A. Pugin, "Montmorillonite under Elevated Pressure and Temperature Conditions," Geokhimiya, No. 7, 790–795 (1966).
25. H. E. Roberson and R. W. Lahann, "Smectite to Illite Conversion Rates: Effects of Solution Chemistry," Clays Clay Miner. **29**, 129–135 (1981).
26. D. Eberl and J. Hower, "Kinetics of Illite Formation," Geol. Soc. Am. Bull. **87**, 1326–1330 (1976).
27. D. Eberl, G. Whitney, and H. Khoury, "Hydrothermal Reactivity of Smectite," Am. Mineral. **63**, 401–409 (1978).

28. A. Inoue, "Potassium Fixation by Clay Minerals during Hydrothermal Treatment," Clays Clay Miner. **31**, 81–91 (1983).
29. A. Inoue, B. Velde, A. Meunier, and G. Touchard, "Mechanism of Illite Formation during Smectite-to-Illite Conversion in a Hydrothermal System," Am. Mineral. **73**, 1325–1334 (1988).
30. R. W. Lahann and H. E. Roberson, "Dissolution of Silica from Montmorillonite: Effect of Solution Chemistry," Geochim. Cosmochim. Acta **44**, 1937–1943 (1980).
31. A. Inoue, "Mechanism of Smectite-to-Illite Transformation," J. Miner. Soc. Jap. **19**, 53–61 (1990).
32. J. J. Howard and D. M. Roy, "Development of Layer Charge and Kinetics of Experimental Smectite Alteration," Clays Clay Miner. **33**, 81–88 (1985).
33. S. J. Köhler, F. Dufaud, and E. H. Oelkers, "An Experimental Study of Illite Dissolution Kinetics as a Function of pH from 1.4 to 12.4 and Temperature from 5 to 50°C," Geochim. Cosmochim. Acta **67**, 3583–3594 (2003).
34. S. Köhler, D. Bosbach, and E. H. Oelkers, "Do Clay Mineral Dissolution Rates Reach Steady State?," Geochim. Cosmochim. Acta **69**, 1997–2006 (2005).
35. G. J. Ross, "Kinetics of Acid Dissolution of an Orthochlorite Mineral," Can. J. Chem. **45**, 3031–3034 (1967).
36. H. Kodama and M. Schnitzer, "Dissolution of Chlorite Minerals by Fulvic Acid," Can. J. Soil Sci. **53**, 240–243 (1973).
37. H. Sverdrup, *The Kinetics of Base Cation Release Due to Chemical Weathering* (Lund Univ. Press, Lund, 1990).
38. H. M. May, J. G. Acker, J. R. Smyth, et al., "Aqueous Dissolution of Low-Iron Chlorite in Dilute Acid Solutions at 25°C," Clay Miner. Soc. Prog. Abstr. **32**, 8819 (1995).
39. C. A. Rochelle and K. Bateman, R. MacGregor, et al., "Experimental Determination of Chlorite Dissolution Rates," in *Materials Research Society Symposium, No. 353. Scientific Basis for Nuclear Waste Management*, Ed. by T. Murakami and R. C. Ewing (1996), pp. 149–156.
40. M. Hamer, R. C. Graham, C. Amrhein, and K. N. Bozhilov, "Dissolution of Ripidilite (Mg, Fe-Chlorite) in Organic and Inorganic Acid Solutions," Soil Sci. Soc. Am. J. **67**, 654–661 (2003).
41. F. Brandt, D. Bosbach, E. Krawczyk-Barsch, et al., "Chlorite Dissolution in the Acid pH-Range: A Combined Microscopic and Macroscopic Approach," Geochim. Cosmochim. Acta **67**, 1451–1461 (2003).
42. A. B. Gustafsson and I. Puigdomenech, "The Effect of pH on Chlorite Dissolution Rates at 25°C," Mat. Res. Symp. Proc. **757**, 649–655 (2003).
43. R. T. Lowson, M.-C. J. Comarmond, G. Rajaratnam, and P. L. Brown, "The Kinetic of the Dissolution of Chlorite as a Function of pH at 25°C," Geochim. Cosmochim. Acta **69**, 1687–1699 (2005).
44. M. Malmström, S. Banwart, J. Lewenhagen, et al., "The Dissolution of Biotite and Chlorite at 25°C in the Near Neutral Region," J. Contam. Hydrol. **21**, 201–213 (1996).
45. G. J. Ross, "Structural Decomposition of an Orthochlorite during Its Acid Dissolution," Can. Mineral. **9**, 522–530 (1968).
46. G. J. Ross, "Acid Dissolution of Chlorites: Release of Magnesium, Iron and Aluminium and Mode of Acid Attack," Clays Clay Mineral. **17**, 347–354 (1969).
47. S. U. Salmon and M. E. Malmström, "Mineral Weathering Rates in Mill Tailings from Kristinenberg, Northern Sweden," in *Abstracts of Eleventh Annual Goldschmidt Conference, Houston* (CD-ROM, 2001), Abstract #3375.
48. G. B. Naumov, B. N. Ryzhenko, and I. L. Khodakovskii, *Reference Book on Thermodynamic Values* (Atomizdat, Moscow, 1971) [in Russian].